Journal of Physics: Conference Series **712** (2016) 012029 doi:10.1088/1742-6596/712/1/012029

The binuclear nickel center in the A-cluster of acetyl-CoA synthase (ACS) and two biomimetic dinickel complexes studied by X-ray absorption and emission spectroscopy

P Schrapers[1], S Mebs[1], Y Ilina[2], D S Warner[3], C Wörmann[2], N Schuth[1], R Kositzki[1], H Dau[1], C Limberg[3], H Dobbek[2] and M Haumann[1]*

[1] Department of Physics, Freie Universität Berlin, 14195 Berlin, Germany
[2] Department of Biology, Humboldt-Universität zu Berlin, 10115 Berlin, Germany
[3] Department of Chemistry, Humboldt-Universität zu Berlin, 12489 Berlin, Germany

*E-mail: michael.haumann@fu-berlin.de

Abstract. Acetyl-CoA synthase (ACS) is involved in the bacterial carbon oxide conversion pathway. The binuclear nickel sites in ACS enzyme and two biomimetic synthetic compounds containing a Ni(II)Ni(II) unit (**1** and **2**) were compared using XAS/XES. EXAFS analysis of ACS proteins revealed similar Ni-N/O/S bond lengths and Ni-Ni/Fe distances as in the crystal structure in oxidized ACS, but elongated Ni-ligand bonds in reduced ACS, suggesting more reduced nickel species. The XANES spectra of ACS and the dinickel complexes showed overall similar shapes, but less resolved pre-edge and edge features in ACS, attributed to more distorted square-planar nickel sites in particular in reduced ACS. DFT calculation of pre-edge absorption and $K\beta_{2,5}$ emission features reproduced the experimental spectra of the synthetic complexes, was sensitive even to the small geometry differences in **1** and **2**, and indicated low-spin Ni(II) sites. Comparison of nickel sites in proteins and biomimetic compounds is valuable for deducing structural and electronic differences in response to ligation and redox changes.

1. Introduction

Carbon oxide (CO_x) conversion reactions in biological enzymes are of high interest for potential renewable energy and climate engineering applications. Nickel-containing proteins such as the acetyl-CoA synthase (ACS) are prominently involved in the bacterial CO_x conversion pathway [1]. The active site of ACS denoted A-cluster features a cubane-type [4Fe4S] cluster linked by a cysteine thiolate to a dinickel unit (figure 1A) [2]. The proximal nickel ion (Ni_p) is bridged by two cysteine thiolates to the distal nickel (Ni_d) ligated by two nitrogen atoms from the protein backbone [3]. Spectroscopic studies have suggested that CO-, methyl- and acetyl groups are bound to Ni_p in the catalytic cycle and that an acetyl species is transferred from ACS to coenzyme-A [4, 5]. Ni_d is believed to remain in the Ni(II) state, whereas Ni_p alternates between Ni(0) or Ni(I) and Ni(II) states in the reaction cycle [1-5]. The nickel valence states, as well as the binding motifs of the small molecule ligands in ACS have been investigated by protein crystallography and spectroscopy [1-5], but are not fully established, partly because of resolution limitations or difficult accessibility of intermediates.

Synthetic model chemistry is a valuable approach for exploring possible coordination motifs and electronic configurations of the biological metal sites. Here, two crystallized dinickel complexes, which mimic the first-sphere coordination of the Ni sites in the ACS by mixed N/S-ligation and thiolate bridging, were studied (figure 1B,C). Both compounds comprise a $Ni^{II}(\mu\text{-}S)_2Ni^{II}$ site as

revealed in earlier studies [6]. X-ray absorption and emission spectroscopy (XAS/XES) facilitates molecular fine structure and electronic configuration determination and is sensitive to all valence and spin states of nickel sites [7]. The pre-edge absorption region of the K-edge due to resonant core-level (1s) electron excitation into valence orbitals (core-to-valence transitions, ctv), and the Kß emission region, due to electronic 3p→1s decay (Kß main lines, $K\beta_{1,3}$ and Kß´) or decay from valence levels in the $K\beta_{2,5}$ region (valence-to-core transitions, vtc), bear valuable information on the electronic structure [8-10]. The ctv and vtc features can be calculated using density functional theory (DFT) [8-10]. Here, we combined Ni XAS, Kß XES, and DFT to study the configurations of the nickel sites.

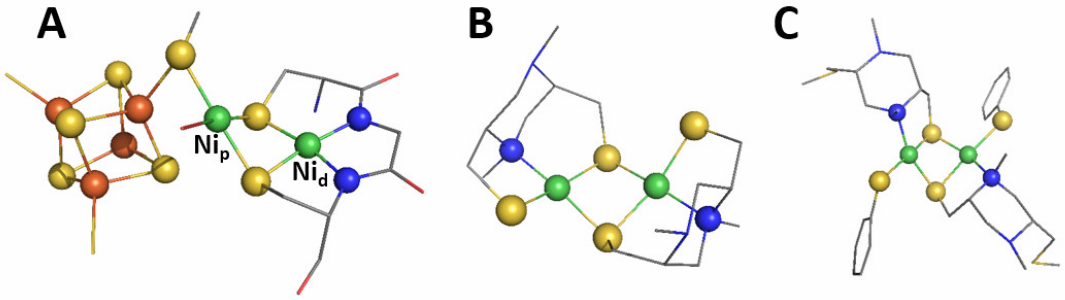

Figure 1. Crystal structures of metal centers in (A) acetyl-CoA synthase (ACS) protein (PDB entry 1RU3, 2.20 Å resolution [3]) and in (B, C) synthetic dinickel complexes (**1**, B [6]; **2**, C, synthesis and crystal data for **2** will be reported in a forthcoming publication). Color code: Ni, green; Fe, orange; N, blue; O, red; S, yellow; C, grey. H-atoms are omitted. Proximal and distal Ni ions in ACS are labelled.

2. Materials and Methods

ACS was purified according to a modified protocol of Svetlichnyi [3, 11]. The ACS gene from *Carboxydothermus hydrogenoformans* was cloned into pET28 with an N-terminal tween-strep tag, which was cleaved with TEV protease over night at RT. Ni-reconstitution was achieved at 45 °C for 48 h (addition of 5 mM ß-ME, 1:2.5 ACS:$NiCl_2$, unbound nickel was removed by gel filtration). As-isolated (oxidized, ACS^{ox}) and titanium(III)-citrate treated (reduced, ACS^{red}) protein samples (~1 mM) were prepared. The nickel complex **1** was synthesized as described in [4], the synthesis of complex **2** will be reported in a forthcoming publication. Metal contents in ACS samples were determined by total-reflection X-ray fluorescence analysis. For ACS, XAS at the Ni K-edge was performed at beamline KMC-1 of the BESSY (Berlin, Germany) using a Si[111] double-crystal monochromator and an energy-resolving 13-element Ge detector for Kα-fluorescence detection. For the Ni complexes, XAS/XES spectra were collected at beamline ID26 of the ESRF (Grenoble, France) using a Si[311] double-crystal monochromator and a vertical-plane Rowland spectrometer with 5 Si[551] analyzer crystals and an avalanche photodiode detector for emission detection. Samples were held in a liquid-He cryostat at 20 K. Single-point DFT calculations on crystal structures of **1** and **2** were performed with the ORCA program [12] (TPSSh functional, TZVP basis set). Calculated spectra were 183 eV shifted on the energy axis, scaled, and broadened by Gaussian (ctv) or Lorentzian (vtc) functions.

3. Results

XAS on ACS protein. Ni XANES and EXAFS spectra of oxidized and reduced ACS samples are shown in figure 2. The XANES spectra exhibit overall similar shapes, excluding major differences in the nickel ligation. A more pronounced shoulder at ~8337 eV in ACS^{ox} and a ~1 eV lowered edge energy in ACS^{red} were observed, the edge downshift presumably reflecting more reduced nickel ions in ACS^{red}. EXAFS fit analysis of ACS^{ox} revealed about 2 Ni-S bonds of ~2.20 Å, 1 Ni-S bond of ~2.60 Å, and 1-2 Ni-N/O bonds of ~1.98 Å. Metal-metal interactions of ~2.91 Å (Ni-Ni) and ~2.69 Å (Ni-Fe) contributed relatively weakly to the EXAFS (~0.5 Ni-Ni/Fe distances per Ni ion). For ACS^{red}, similar coordination numbers, but overall slightly longer distances were found (Ni-S, ~2.24 Å/~2.62 Å; Ni-N/O, ~1.99 Å; Ni-Ni/Fe, ~2.98 Å and ~2.64 Å). The Fe/Ni ratio of ~3 for the ACS samples was larger than the ratio of 2 for a [4Fe-4S]-Ni-Ni cluster, suggesting sub-stoichiometric Ni contents.

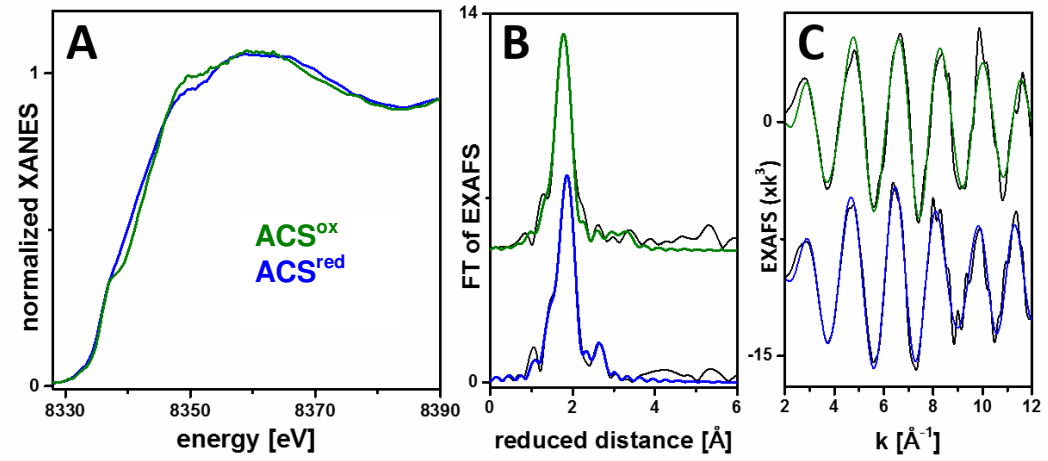

Figure 2. Ni XAS spectra of ACS proteins. (A) XANES spectra, (B) Fourier-transforms of EXAFS spectra in (C) (black lines, experimental data; colored lines, simulations with parameters given in the text). Spectra are vertically shifted in (B) and (C) for comparison.

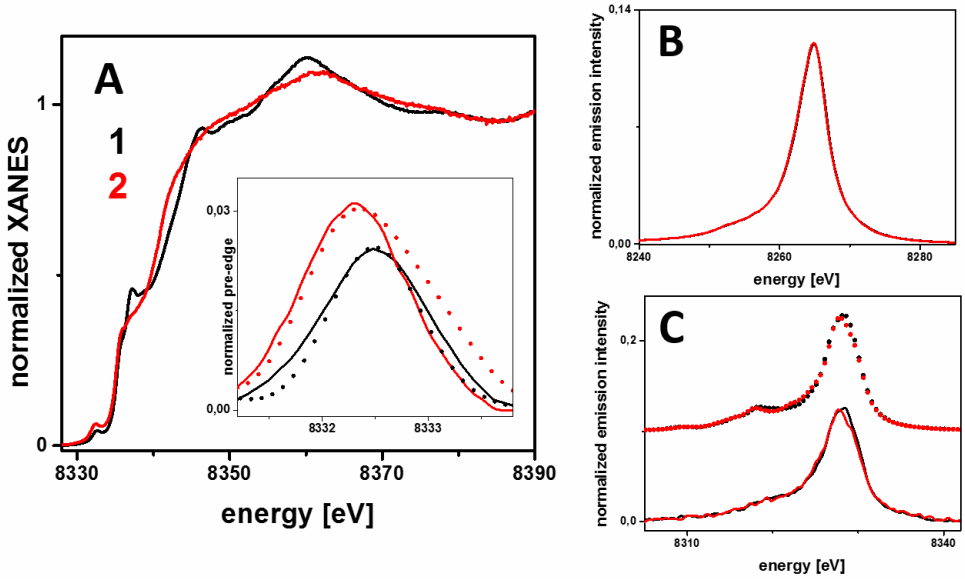

Figure 3. XAS/XES spectra of two synthetic dinickel complexes. (A) XANES spectra and isolated pre-edge features (ctv) in the inset (lines, experimental data; dots, DFT-calculated spectra), (B) Kß main line emission, (C) $K\beta_{2,5}$ emission lines (vtc; bottom, experimental data; top, spectra from DFT).

XAS/XES on dinickel complexes. Both synthetic compounds show XANES shapes resembling the ACS spectra, but revealing better resolved features due to less distorted square-planar Ni sites in the complexes (figure 3). The more pronounced shoulder (at ~8337 eV) in the XANES of **1** is associated with a ~0.4 Å larger Ni-Ni distance and more regular site symmetries compared to **2**. This suggested a more distorted site symmetry also in ACS^{red} compared to ACS^{ox}. Complexes **1** and **2** showed a discernable pre-edge feature (~8332.5 eV), as explained by considerable admixtures of molecular orbitals with ligand character to the Ni(d) valence levels, whereas a pre-edge feature was hardly resolved in the ACS spectra. Both complexes showed almost identical Kß main line spectra with dominant $K\beta_{1,3}$ (~8265 eV) and small Kß´ (~8255 eV) features due to similar low-spin Ni(II)Ni(II) states ([4], manuscript in preparation). Also the $K\beta_{2,5}$ emission lines were alike, reflecting the similar coordination environment and electronic structure of the Ni sites in both complexes. Calculation by DFT of the pre-edge absorption (ctv) and $K\beta_{2,5}$ emission (vtc) spectra based on the crystal structures of **1** and **2** accordingly yielded good agreement with the experimental data only for low-spin Ni(II) sites.

4. Discussion

We compared the dinickel units in ACS protein and two biomimetic complexes. The nickel-ligand bond lengths and metal-metal distances of ACS in solution were similar to the single-crystal structure, suggesting similar site configurations. Significant reduction of the nickel in ACS manifested in a K-edge energy down-shift and considerable Ni-N/O/S bond elongation, possibly due to formation of mixed-valence Ni(I)Ni(II) species in the reduced enzyme compared to a Ni(II)Ni(II) unit in oxidized ACS. The apparent relatively small contributions to the EXAFS of Ni-Ni/Fe interactions, which are expected according to the crystal structure [3], presumably are explained by incomplete nickel reconstitution (sub-stoichiometric Ni contents) in the ACS protein, by admixtures of (inactive) Ni-Zn sites, and by destructive interference of counterphasic EXAFS oscillations of Ni-Ni/Fe and long Ni-S interactions as also observed for other nickel enzymes [13]. The XANES spectral similarities of ACS and the models suggest overall similar square-planar Ni(II)Ni(II) site geometries, which are considerably more distorted in the ACS. In particular, the pre-edge absorption feature reflecting resonant core-to-valence excitations was less resolved in ACS, as explained in part by monochromator resolution differences, but also site symmetry variations and/or the presence of different active site species in the oxidized and reduced protein samples may be involved. Kß XES and DFT calculations of ctv and vtc spectra confirmed the low-spin Ni(II) centers in **1** and **2**. The spin-state of the nickel sites in ACS remains to be addressed using Kß XES. These results show that comparison of XAS/XES data of biological and synthetic dinickel centers provides access to molecular and electronic structure differences. Further work on the ACS protein along this line is in progress in our laboratories.

Acknowledgments

M.H., H.Do., H.Da., and C.L. gratefully acknowledge support within Unicat (Cluster of Excellence Berlin). M.H. thanks the Deutsche Forschungsgemeinschaft for a Heisenberg Fellowship and for funding (grant Ha3265/6-1) and the Bundesministerium für Bildung und Forschung for support within the Röntgen-Angström Cluster (grant 05K14KE1). We thank the groups of P. Glatzel at ID26 of ESRF and of F. Schäfers at KMC-1 of BESSY (Helmholtz Center Berlin) for excellent technical support.

References

[1] Appel A M, Bercaw J E, Bocarsly A B, Dobbek H, DuBois D L, Dupuis M, Ferry J G, Fujita E, Hille R, Kenis P J, Kerfeld C A, Morris R H, Peden C H, Portis A R, Ragsdale S W, Rauchfuss T B, Reek J N, Seefeldt L C, Thauer R K and Waldrop G L 2013 *Chem. Rev.* **113** 6621
[2] Jeoung J H, Goetzl S, Hennig S E, Fesseler J, Wörmann C, Dendra J and Dobbek H 2014 *Biol. Chem.* **395** 545
[3] Svetlitchnyi V, Dobbek H, Meyer-Klaucke W, Meins T, Thiele B, Römer P, Huber R and Meyer O 2004 *Proc. Natl. Acad. Sci. U. S. A.* **101** 446
[4] Barondeau D P and Lindahl P 1997 *J. Am. Chem. Soc.* **119** 3959
[5] Seravalli J, Kumar M and Ragsdale S W 2002 *Biochemistry* **41** 1807
[6] Warner D S, Limberg C and Mebs S 2013 *Z. Anorg. Allg. Chem.* **639** 1577
[7] Haumann M (2015) In *Biohydrogen* (Rögner M, Ed), DeGruyter, Berlin, 97
[8] Lambertz C, Chernev P, Klingan K, Leidel N, Siegfridsson K G V, Happe T and Haumann M 2014 *Chem. Sci.* **5** 1187
[9] Chernev P, Lambertz C, Brünje A, Leidel N, Sigfridsson K G V, Kositzki R, Hsieh C H, Yao S, Schiwon R, Driess M, Limberg C, Happe T and Haumann M 2014 *Inorg. Chem.* **53** 12164
[10] Leidel N, Chernev P, Havelius K G V, Schwartz L, Ott S and Haumann M 2012 *J. Am. Chem. Soc.* **134** 14142
[11] George S J, Seravalli J and Ragsdale S W 2005 *J. Am. Chem. Soc.* **127** 13500
[12] Neese F 2012 *Wiley Interdisc. Rev. Comput. Mol. Sci.* **2** 73
[13] Sigfridsson K G V, Leidel N, Sanganas O, Chernev P, Lenz O, Yoon K S, Nishihara H, Parkin A, Armstrong F A, Dementin S, Rousset M, De Lacey A L and Haumann M 2015 *Biochim. Biophys. Acta* **1847** 162